

# **Pb–Zn–Cd–As Pollution in Soils Affected by Mining Activities in Central and Southern Spain: A Scattered Legacy Posing Potential Environmental and Health Concerns**

1  
2  
3  
4

AUI

**Javier Lillo, Roberto Oyarzun, José María Esbrí,  
Mari Luz García-Lorenzo, and Pablo Higuera**

5  
6

**Abstract** In this chapter, published geochemical data for soils from several Pb–Zn 7  
mine sites and districts from Spain are reviewed. Although most of the mines have 8  
closed down, a legacy of highly polluted soils still remains throughout the sites 9  
constituting a potential hazard for the environment and human health. The fate of 10  
the studied metals and metalloids in these soils is mainly controlled by factors such 11  
as mining methods, concentration and metallurgical operations, mineralogy of the 12  
ore, gangue and host rock, fracturing of the host rocks, physiography, climate, and 13  
soil types (pedogenic evolution). It can be concluded that the most polluted soils 14  
(identified on the basis of an enrichment factor) are those of the Sierra Minera 15  
(La Unión District – SE Spain), at more than 488 (Pb), 163 (Zn), 99 (Cd), and 16  
98 (As) times the background values from non-contaminated soils. Pb is usually 17  
related to As, which in turn is bound to Fe oxides and oxyhydroxides. Metal bearing 18  
jarosite and other soluble phases also play a relevant role in the studied soil–water 19

---

J. Lillo (✉)

Departamento de Biología, Geología, Física y Química Inorgánica, ESCET, Universidad Rey  
Juan Carlos, 28029 Móstoles, Madrid, Spain

IMDEA Water Inst., Parque Científico Tecnológico de la Universidad de Alcalá, 28805 Alcalá  
de Henares, Madrid, Spain

e-mail: [javier.lillo@urjc.es](mailto:javier.lillo@urjc.es)

R. Oyarzun

Departamento de Cristalografía y Mineralogía, Facultad de Ciencias Geológicas, Universidad  
Complutense, 28040 Madrid, Spain

J.M. Esbrí and P. Higuera

Instituto de Geología Aplicada-Área de Explotación de Minas, Universidad de Castilla-La  
Mancha, 13400 Almadén (Ciudad Real), Spain

M.L. García-Lorenzo

Departamento de Petrología y Geoquímica, Facultad de Ciencias Geológicas, Universidad  
Complutense, 28040 Madrid, Spain

20 systems, because these minerals are dissolved during intense rainy events, thus  
21 resulting in high rates of metal leaching and mobilization by runoff.

22 **Keywords** Arsenic, Environmental geochemistry, Iberian Peninsula, Metals,  
23 Mine sites, Soils

## 24 Contents

25	1	A Brief Revision of the Most Relevant Pb–Zn Ore Deposits from the Southern and Central Iberian Peninsula
26	1.1	Variscan Age Ore Deposits and Districts
27	1.2	Alpine Age Ore Deposits and Districts
28	2	Understanding of the Geochemical Behavior of Pb and Zn in Natural Environments
29	2.1	Environmental Mineralogy and Geochemistry of Pb and Zn: A Brief Introduction
30	2.2	Speciation of Pb and Zn in Contaminated Soils
31	3	Mining and Pb–Zn Dispersion in Soils: Some Facts and Fads
32	3.1	How Bad Is the Case?
33	3.2	When Should We (Really) Worry About?
34	4	Pb, Zn, Cd, and As in Soils from the Studied Iberian Mining Sites and Districts
35	4.1	Mean Concentrations
36	4.2	Enrichment Factors (REF <sub>metal</sub> )
37	4.3	Correlations and Clustering of Data
38	5	Conclusions
39		References

## Abbreviations

40	A	Agricultural
41	AFS	Atomic fluorescence spectroscopy
42	AMD	Acid mine drainage
43	BDL	Below detection limit
44	EDXRF	Energy dispersive X-ray fluorescence
45	ETAAS	Electrothermal atomization atomic absorption spectrometry
46	FAAS	Flame atomic absorption spectrometry
47	ICP-AES	Inductively coupled plasma atomic emission spectroscopy
48	ICP-MS	Inductively coupled plasma mass spectrometry
49	INAA	Instrumental neutron activation analysis
50	IPB	Iberian Pyrite Belt
51	MCL	Maximum contaminant levels
52	Q1	First quartile
53	Q3	Third quartile
54	REF <sub>metal</sub>	Relative enrichment factor
55	RPL	Residential or parkland

<b>1 A Brief Revision of the Most Relevant Pb–Zn Ore Deposits from the Southern and Central Iberian Peninsula</b>	56
	57
	58

Given that this chapter is focused on metal pollution and Pb–Zn mineral deposits from the Iberian Peninsula, it is worth mentioning here that metal (and metalloid) dispersion can have both a natural and industrial origin. In this regard, once a mineral deposit is in the surface or near surface environment, fracturing will result in increased permeability and, therefore, in enhanced movement of oxygen-rich meteoric solutions throughout the ore bodies. This implies higher rates of oxidation and metal leaching. This case can be understood in terms of natural (geological) metal pollution. The second case is far more obvious and relates to the mining, processing, and smelting of Pb–Zn sulfides. Thus, to fully understand the combination of natural and industrial, a concise geological revision of the studied mine sites and districts follows.

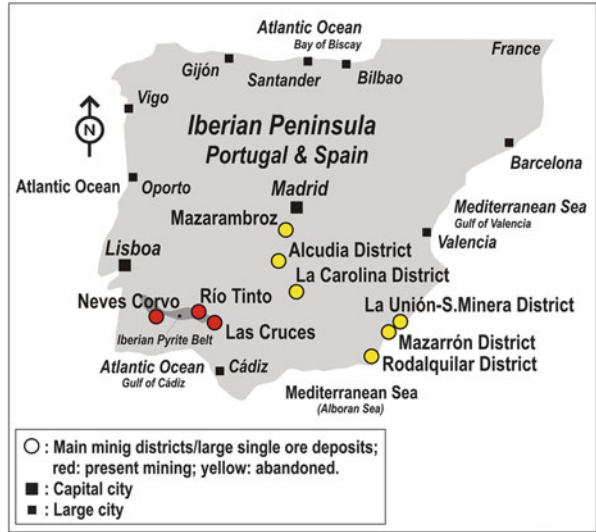
There are numerous Pb–Zn ore deposits in southern and central Spain (Fig. 1), and these formed in different geological scenarios throughout the Iberian Peninsula from Paleozoic to Cenozoic time. With the exception of a few ore deposits in the Iberian Pyrite Belt (e.g., Las Cruces in Spain, Neves Corvo in Portugal), all mining operations in the described districts have ceased. However, a legacy of tailings deposits, waste rock dumps, and highly polluted soils still remains there constituting a potential hazard for the environment and public health.

### **1.1 Variscan Age Ore Deposits and Districts** 77

These ore deposits are Pb–Zn hydrothermal vein deposits of Variscan to late Variscan age emplaced along faults crosscutting metasedimentary sequences of Neoproterozoic to Silurian age:

- Alcudia Valley and the San Quintín mining group, southern–central Spain (Fig. 1, Table 1), with about 453 ore deposits (most of them are of very small size). Total Pb production from the Alcudia Valley has been estimated at 1.4 Mt, of which 1.25 Mt was produced between 1840 and 1988. Estimated Ag production was 350 t. Lack of data prevents a reliable estimation of Zn production. For more info, see the comprehensive paper of Palero et al. [1]. Environmental impact: minor and very localized [2]. However, tailings deposits and acid mine drainage (AMD) may pose an environmental hazard for surrounding agricultural lands such as at the San Quintín mining group [3].
- Py–(Cu)–Zn–Pb–(Sn) stockwork and stratiform massive sulfides of volcanogenic origin and Upper Famennian–Lower Viséan age occur in southern Portugal and Spain defining the so-called Iberian Pyrite Belt (IPB) (Fig. 1, Table 1), with more than 80 known deposits containing 1,700 Mt of sulfides

Fig. 1 Location of the Pb–Zn mining districts considered in this chapter



94 (250 Mt have been extracted; [25]), amounting 14.6 Mt Cu, 13 Mt Pb, 34.9 Mt  
 95 Zn, 46,100 t Ag, and 880 t Au. For more info on the belt, see the comprehensive  
 96 paper of Leistel et al. [9]. A few mines are currently operating along the belt,  
 97 e.g., Las Cruces (Spain) and Neves Corvo (Portugal). Environmental impact:  
 98 huge, including complete degradation of the River Tinto which owes its deep red  
 99 color (and name) to massive AMD. The high pollution by heavy metals affecting  
 100 the soils of the IPB deserved a noteworthy number of studies (e.g., [10–12]). The  
 101 good news is that the red color is a tourist attraction and the river serves as a  
 102 world-class natural laboratory for the study of specialized algae and bacteria  
 103 (e.g., [18]).

- 104 • The Linares–La Carolina Ba–Pb–Zn–Cu–(Ag) vein deposits in central Spain  
 105 (Fig. 1, Table 1) were mainly mined in the period 1875–1920 and constituted one  
 106 of the most outstanding mining districts of Europe, with an average lead  
 107 production of 65,000 t year<sup>-1</sup> and up to 500 g/t silver obtained as a  
 108 by-product. The workings were concentrated on vein-type hydrothermal mineral-  
 109 alization hosted by granitoids and metasediments. The El Cobre vein, a cordil-  
 110 leran vein-type deposit, is representative of the veins in the district and is also  
 111 one of the largest. The vein strikes northeast–southwest for about 5 km, has an  
 112 average thickness of 2–3 m, and is hosted by monzogranitic rocks (the so-called  
 113 Monzogranito de Linares) and minor Carboniferous metasediments. For more  
 114 info on this district, see the paper of [5]. The soils of the district [6] are extremely  
 115 rich in Pb (up to 410 times the world average for soils, [26]) whereas for Zn the  
 116 enrichment is much lower (up to 7 times the world average for soils [26]).

**Table 1** Summary of basic information (ore and gangue, soils, and climate) from the districts considered in this chapter. Main references have been included

	District	Metal association/ore type/main ore/gangue mineralogy	Soil uses/types/parent material	Climate	References
t.1					
t.2					
t.3	Alcudia, San Quimín	Pb-Zn-(Cu)-(Ag) Vein-type deposits Sulfides, sulfosalts Quartz, ankerite, siderite, barite, calcite	<i>Dehesa</i> pastures (clear forest of evergreen oaks), Mediterranean forest Soil parent material <sup>13</sup> : metasediments	Mediterranean (dry season from June to September, average annual temperature is 14–15°C, average annual precipitation is 430–550 mm)	[1–4]
t.4	Linares-La Carolina	Ba-Pb-Zn-Cu-(Ag) Vein-type deposits Sulfides, sulfosalts Quartz, ankerite, barite, calcite,	<i>Dehesa</i> pastures, agriculture (olive groves, minor cereal crops) Soil parent material <sup>14</sup> : granites, metasediments, sedimentary rocks (sandstones, lutites, and marls)	Mediterranean (dry season from June to September, average annual temperature is 17°C, average annual precipitation is ~470 mm)	[5–8]
t.5	Iberian Pyrite Belt (IPB)	Py-(Cu)-Zn-Pb-(Sn) Stockwork and stratiform massive deposits, Gossans Sulfides Silicates (quartz, chlorite, sericite), carbonates, barite	Degraded scrub, forest scrub, agriculture (orange plantations, horticulture), reclaimed for forest land Entisols Soil parent material <sup>14</sup> : shales, volcanic and volcanic-sedimentary rocks	Semi-arid Mediterranean (xeric-aridic moisture regime, dry season from April to September, average annual temperature is 15–20 °C, average annual precipitation is 400–700 mm)	[9–11]; IPB2 data set [12]; IPB1 data set [13]
t.6	Mazarambroz	Pb-Zn-(Ag) Vein-type deposits Sulfides, minor sulfosalts Quartz, siderite, barite	<i>Dehesa</i> pastures (clear forest of evergreen oaks), agriculture (extensive cereal crops) Cambisols, Anthrosols Soil parent material <sup>14</sup> : granites, migmatites, metasediments	Mediterranean (dry season from June to September, average annual temperature is ~16°C, average annual precipitation is ~370 mm)	[14–16]
t.7	Mazarrón	Pb-(Ag)-Zn-(As) Vein and stockwork type Sulfides Quartz, calcite, siderite, dolomite, and gypsum	Degraded scrub Anthrosols Soil parent material: volcanic rocks (dacites and rhyodacites)	Semi-arid Mediterranean (dry season from June to August, average annual temperature is 16.5–18.8 °C, average annual precipitation is 185–310 mm)	[17]
t.8					[18–22] (continued)

t.9 **Table 1** (continued)

District	Metal association/ore type/main ore/gangue mineralogy	Soil uses/types/parent material	Climate	References
t.10 La Unión (Sierra Minera, Cartagena)	Pb-(Ag)-Zn-(Sn)-(As) Stratabound ore deposits, disseminations in sedimentary facies, stockworks, Gossans Sulfides, sulfosalts Quartz, carbonates, clays, chlorite, sulfates	Degraded scrub, agriculture? Anthrosols Soil parent material <sup>a</sup> : sedimentary rocks (sands and conglomerates), subvolcanic (rhyolite, dacite, and andesite) and volcanic (alkaline basalt)	Semiarid Mediterranean (dry season from June to August, average annual temperature is 17°C, average annual precipitation is ~300 mm)	
t.9 Rodalquilar	High-sulfidation-type Au-(As)-alunite vein deposits Peripheral low-sulfidation Pb-Zn-Cu-(Au) veins Sulfides, sulfosalts Quartz, clays, alunite, chlorite	Degraded scrub, agriculture Inceptisols, Anthrosols Soil parent material <sup>a</sup> : ignimbrites, felsic domes	Semiarid Mediterranean (dry season from May to August, average annual temperature is 18°C, average annual precipitation is 200 mm)	[23, 24]

t.10 <sup>a</sup>In addition to mine wastes and modern sediments

## 1.2 Alpine Age Ore Deposits and Districts

117

- The Mazarrón district mineral deposits (SE Spain) (Fig. 1, Table 1) formed in Miocene time in relation to the emplacement of dacitic–rhyodacitic domes. The Pb–(Ag)–Zn–(As) ore deposits are of vein and stockwork type. There are three main mining sites (from east to west): San Cristóbal–Perules (adjacent to the town of Mazarrón), Pedreras Viejas, and Coto Fortuna. The area is located in the southern realm of a Miocene–Pliocene marine basin surrounded by mountains in its western, eastern, and southern flanks. The mines were exploited for lead, silver, and zinc during the nineteenth to twentieth centuries (until the early 1960s). The latter corresponds to the peak period of mineral extraction when 3 Mt of ore at 10% Pb and 150 g t<sup>-1</sup> Ag was extracted between 1920 and 1941. This was followed by a decline in the period 1951–1962, when only 1 Mt of ore at 3% Pb, 5% Zn, and 115 g t<sup>-1</sup> Ag was extracted. Despite strong AMD (seasonal ponds) and extremely high contents of Pb and Zn (and As) in the tailings and soils, ionic metal migration is limited by the presence of carbonate rocks (Alpujárrides Complex) and soils. The anthropic soils of the district are extremely rich in Pb (up to 200 times the world average for soils, [26]), whereas for Zn the enrichment is lower (up to 80 times the world average for soils, [26]). However, some extremely metal-rich tailings deposits reach the Las Moreras seasonal stream. For more info on this district, see Oyarzun et al. [17].
- The La Unión–Sierra Minera Pb–(Ag)–Zn–(Sn)–(As) district in Cartagena (SE Spain) (Fig. 1, Table 1) hosts ore deposits of different types, having in common a late Miocene age. These include stratabound ore deposits (the so-called mantos) (e.g., Emilia, Brunita), disseminations in the Miocene marine facies (e.g., Sultana), stockworks in felsic domes (e.g., Cabezo Rajao), and gossans. The mining district covers an area of about 10 × 5 km<sup>2</sup> that contains one of the largest densities of Pb–Zn ore deposits in Spain. Modern mining at the Sierra de Cartagena can be divided into two periods. The first one comprised traditional, underground operations that were active until the early 1950s. From 1957 onwards the Sociedad Minero Metalúrgica Peñarroya España (a French mining group) began large open pit mining operations, which led first to the generation of large volumes of tailings and mineral dumps and eventually to huge abandoned pits. The Roberto froth flotation plant disposed directly onto the Portman bay about 60 Mt of tailings during the period 1957–1990, eventually making the shoreline advance between 500 and 600 m seaward [19]. For more info on the district, see López\_García et al. [18]. A myriad of tailings and waste rock deposits (nineteenth and twentieth centuries) are scattered throughout the district, although metal dispersion is restricted by the presence of carbonate rocks (Alpujárrides Complex) and soils. However, the area affected by mining activities is not small and covers about 1,000 km<sup>2</sup> [20]. Besides, agricultural soils surrounding old mining works (e.g., Cabezo Rajao) may have up to 2,000 mg kg<sup>-1</sup> Pb and 1,200 mg kg<sup>-1</sup> Zn [21].

AU2

AU3

- 159 • The Rodalquilar district in Almería (SE Spain) (Fig. 1, Table 1) is well known  
160 for its high-sulfidation-type Au–(As)–alunite vein deposits within a large volca-  
161 nic caldera of Miocene age, with an ore mineralogy consisting of native gold  
162 ( $\text{Au}^0$ ), pyrite, enargite ( $\text{Cu}_3\text{AsS}_4$ ), tennantite ( $\text{Cu}_{12}\text{As}_4\text{S}_{13}$ ), tetrahedrite  
163 ( $\text{Cu}_{12}\text{Sb}_4\text{S}_{13}$ ), cinnabar ( $\text{HgS}$ ), bismuthinite ( $\text{Bi}_2\text{S}_3$ ), cassiterite ( $\text{SnO}_2$ ), galena,  
164 and sphalerite. However, the district also hosts peripheral low-sulfidation Pb–  
165 Zn–Cu–(Au) veins. The geological setting of Rodalquilar district includes Upper  
166 Miocene felsic domes, ignimbrites, ash fall deposits, massive volcanic rocks,  
167 and a limestone complex of Messinian age. The sulfide mineralogy of the  
168 peripheral low-sulfidation deposits consists of native gold, sphalerite, galena,  
169 chalcopyrite, and pyrite. Mining initiated around 1825 for Pb, Zn, and Cu, and it  
170 was not until 1864 that the miners realized that the ore contained some gold as  
171 well. Mining operations belonging to this period are those of Consulta, María  
172 Josefa, San Diego, and Triunfo. The larger mining operation relates to the El  
173 Cinto high-sulfidation deposits and took place between 1943 and 1966, when  
174 about 1.6 Mt of ore grading  $3.5 \text{ g t}^{-1}$  Au was extracted. Most if not all of the  
175 tailings (between 900,000 and 1,250,000  $\text{m}^3$ ) around the town of Rodalquilar can  
176 be related to this mining period. For more info on the district, see the papers of  
177 Arribas et al. [23] and Oyarzun et al. [24]. Main environmental concerns relate to  
178 the high contents of As in anthropic and agricultural soils.
- 179 • The Mazarambroz Pb–Zn mineralization in the Toledo Mountains (central  
180 Spain) (Fig. 1, Table 1) is filling E–W fractures following the main direction  
181 of the so-called Mylonitic Band of Toledo. The veins are hosted by migmatites,  
182 metasediments, and granitic rocks related to the Mora Plutón [14]. Ag-rich  
183 galena and sphalerite are the main ore minerals, being accompanied by arseno-  
184 pyrite ( $\text{FeAsS}$ ), pyrite and marcasite ( $\text{FeS}_2$ ), chalcopyrite ( $\text{CuFeS}_2$ ), and  
185 gersdorffite ( $\text{NiAsS}$ ), with quartz ( $\text{SiO}_2$ ), siderite ( $\text{FeCO}_3$ ), and barite ( $\text{BaSO}_4$ )  
186 as the dominant gangue minerals [15]. Mines in this area were exploited until the  
187 late 1970s [15]. The soils in this area show Pb, Zn, and As concentrations much  
188 higher than the regional averages for soils [16].

## 189 2 Understanding of the Geochemical Behavior of Pb 190 and Zn in Natural Environments

### 191 2.1 Environmental Mineralogy and Geochemistry of Pb 192 and Zn: A Brief Introduction

193 Lead and zinc are base metals that form one of the classic associations in ore  
194 deposits. Galena ( $\text{PbS}$ ) and sphalerite ( $\text{ZnS}$ ) are their common sulfide minerals, and  
195 they can be found together with chalcopyrite ( $\text{CuFeS}_2$ ), pyrite ( $\text{FeS}_2$ ), and arseno-  
196 pyrite ( $\text{FeAsS}$ ) (among others) in a variety of geological and ore-forming settings,  
197 such as skarns in limestones and dolostones (dolomites), hydrothermal veins, and

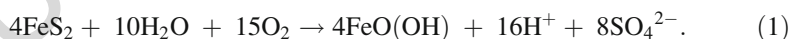


replacements in plutonic or volcanic rocks of felsic composition, volcanogenic massive sulfide deposits, and Mississippi Valley-type Pb–Zn ore deposits. Other common lead and zinc minerals are anglesite (PbSO<sub>4</sub>), cerussite (PbCO<sub>3</sub>), and smithsonite (ZnCO<sub>3</sub>), together with the less common willemite (Zn<sub>2</sub>SiO<sub>4</sub>) and zincite (ZnO). The presence of silver in galena (either as mineral inclusions or solid solution) is relatively common.

The environmental legislation of most countries has progressively retired lead from common uses such as plumbing, additives for petrol, and paints, while it remains nevertheless being widely used in lead–acid batteries for cars. On the other hand, the major environmental and health concerns regarding Zn are not strictly related to the element but to its most common mineral: sphalerite, which usually hosts Cd. Cadmium and zinc belong to the same group of the periodic table (IIB) and share chemical properties such as the tetrahedral covalent bond and other crystal structures. They have similar ionic radii: Zn<sup>2+</sup> (0.74 Å) and Cd<sup>2+</sup> (0.97 Å), which accounts for the observation that cadmium occurs in sphalerite as an isomorphous impurity [27].

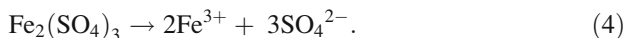
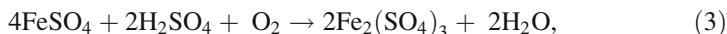
Lead and zinc ([28, 29]) can be regarded as chalcophile (i.e., those elements that combine easily with sulfur) although Zn also has lithophile affinities (i.e., those elements that concentrate in the silicate phase and combine readily with oxygen in the Earth's crust). The solubility of their ionic species (Pb<sup>2+</sup>, Zn<sup>2+</sup>) is controlled by the ionic potential, being extremely high in the case of Zn or extremely low in the case of Pb, which will form insoluble sulfates or carbonates (PbSO<sub>4</sub>, PbCO<sub>3</sub>). This is crucial to understand their geochemical behavior in the environment because while Pb will remain close to the source, Zn can move and disperse easily. This will happen even in extremely dry scenarios such as the Atacama Desert, where Zn forms vast geochemical halos surrounding the source (e.g., [30]).

Pb in freshwater systems will be complexed by carbonate species (Pb(CO<sub>3</sub>)<sub>2</sub><sup>2-</sup>) at pH 6–8, whereas stable species below and above this range will be PbSO<sub>4</sub> (or Pb<sup>2+</sup> in low-sulfate waters) and Pb(OH)<sub>2</sub>, respectively [26]; besides, Zn<sup>2+</sup> is the most stable species of zinc below pH 8, whereas ZnCO<sub>3</sub> is stable at higher pH. Complexing of Zn with SO<sub>4</sub><sup>2-</sup> becomes important only in sulfate-rich acidic waters [26], a geochemical scenario where important oxidation of pyrite (FeS<sub>2</sub>) has occurred (1) leading to formation of AMD:

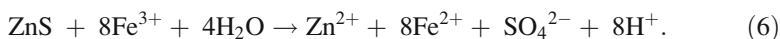
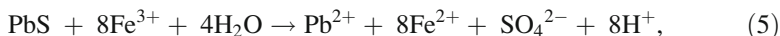


This is also important to understand oxidation and hydrolysis of galena and sphalerite in the supergene environment of the higher sections of sulfide ore deposits (2, 3), because if pyrite is volumetrically unimportant, reaction (4) will be insignificant and no important formation of Fe<sup>3+</sup> will occur [31]:

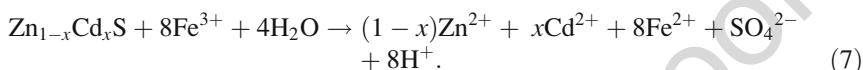




235 The chemical evolution of the system from (2) to (4) is the main prerequisite to  
236 induce oxidation and hydrolysis of galena (5) and sphalerite (6) [31]:



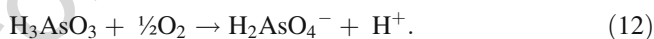
237 Given that sphalerite often contains Cd, the oxidation and leaching of this metal can  
238 be expressed in the following way (7):



239 Arsenopyrite is present in many Pb–Zn deposits (e.g., the Mazarrón district),  
240 and therefore it is worth showing here how the oxidation of this mineral occurs  
241 [32] (8–11):

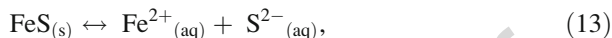


242 If  $f\text{O}_2$  conditions are high, then oxidation of  $\text{As}^{3+}$  to  $\text{As}^{5+}$  may proceed in the  
243 following way [33] (12):

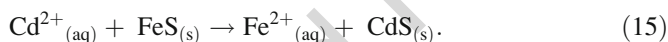


244 The concentrations of these ionic or complex ion species in water are a particularly  
245 sensitive case regarding public health; in this regard, maximum contaminant levels  
246 (MCLs) for drinking water (USA) for these elements are Pb ( $0.015 \text{ mg L}^{-1}$ ), Zn  
247 ( $5 \text{ mg L}^{-1}$ ), Cd ( $0.005 \text{ mg L}^{-1}$ ), and As ( $0.01 \text{ mg L}^{-1}$ ) [34]. MCLs have to be  
248 understood as the highest level of a contaminant that is allowed in drinking water  
249 using the best available treatment technology and taking cost into consideration  
250 [34]. However, do these MCL figures reveal the complete picture regarding metal  
251 toxicity? Not really, because toxicity does not depend on concentration but on the  
252 bioavailability of the metal species [35]. In fact, strongly complexed metals,  
253 especially those complexed by natural chelating agents such as the humic acids,  
254 appear to be completely unavailable and nontoxic [35]; thus, metal speciation  
255 studies are of paramount importance to fully understand the potential health hazards  
256 derived from the existence of high concentrations of metals in waters (surface or  
257 underground). The same applies to sediments and soils.

Regarding sediment quality guidelines for freshwater ecosystems, the following threshold effect concentrations (meaning that below these levels, no adverse effects for the biota should happen) are suggested for lead, zinc, and cadmium: Pb (35 mg kg<sup>-1</sup>), Zn (121 mg kg<sup>-1</sup>), Cd (0.99 mg kg<sup>-1</sup>), and As (9.79 mg kg<sup>-1</sup>) [36]. Nevertheless, natural systems are to be regarded for what they are, nonlinear highly complex systems in which the outcome cannot be fully predicted based only on the study of just a few variables. For example, the ultimate fate of free cadmium (Cd<sup>2+</sup>) may be strongly influenced by the presence of pyrite, which is particularly important in anoxic media. In this regard, two reactions (13, 14) are to be taken into account [35]:



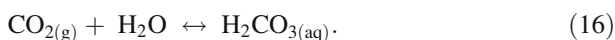
In this regard, if the free (and therefore available) Cd<sup>2+</sup> metal ion is combined with free sulfur (S<sup>2-</sup>), then CdS will precipitate and become unavailable. Given that cadmium has more affinities for sulfur than iron, then the overall reaction will proceed towards the products (right-hand side) (15):



A similar concern regarding these elements is observed in the Canadian Soil Quality Guidelines [37], which indicate maxima levels of (A, agricultural; RPL, residential or parkland): 70 mg kg<sup>-1</sup> (A) and 140 mg kg<sup>-1</sup> (RPL) for Pb, 200 mg kg<sup>-1</sup> (A and RPL) for Zn, 1.4 mg kg<sup>-1</sup> (A) and 10 mg kg<sup>-1</sup> (RPL) for Cd, and 12 mg kg<sup>-1</sup> (A and RPL) for As.

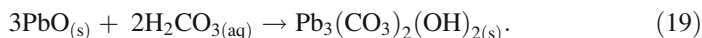
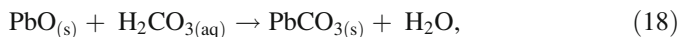
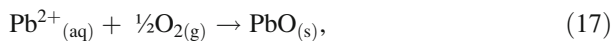
## 2.2 Speciation of Pb and Zn in Contaminated Soils

Speciation of metals in soils depends on the type of soil matrix, pH, Eh, colloidal activity, and climate. For example, in soils with abundant organic matter, Pb<sup>2+</sup> may be complexed to salicylate- and catechol-type functional groups of humic substances [38], whereas Zn is not expected to significantly bind to organic matter [39]. Conversely, Zn<sup>2+</sup> in these acidic soils can be found as franklinite [(Zn, Mn<sup>2+</sup>, Fe<sup>2+</sup>)(Fe<sup>3+</sup>, Mn<sup>3+</sup>)<sub>2</sub>O<sub>4</sub>] or bound by adsorption to Fe and Mn oxyhydroxides as inner-sphere sorption complexes [39]. To understand lead speciation in carbonate-rich soils, the formation of carbonic acid has to be considered since it is a key reactant for the ultimate fate of this metal (16):



Pb<sup>2+</sup> in alkaline soils such as pedocals (which form in semiarid and arid regions) will first form Pb oxides (17), followed by the formation of cerussite (PbCO<sub>3</sub>) (18)

288 at nearly neutral to slightly alkaline pH and even hydrocerussite (19) if pH is high  
289 enough:



290 In the same environment,  $\text{Zn}^{2+}$  may form smithsonite ( $\text{ZnCO}_3$ ) or hydrozincite  
291 ( $\text{Zn}_5(\text{CO}_3)_2(\text{OH})_6$ ).

292 Arsenic is usually bound to Fe oxide/hydroxide phases in soils [33] and river  
293 sediments (e.g., [40]). Colloidal goethite has a net positive charge in acid media  
294 [41], which binds by adsorption of the negatively charged arsenic complex ions of  
295 general composition  $\text{H}_x\text{AsO}_y^{-z}$  (where  $x = 1, 2, \text{ or } 3$ ;  $y = 3 \text{ or } 4$ ; and  $z = 0, -1, \text{ or}$   
296  $-2$ ). These complex ions may remain strongly bound to goethite up to higher pH of  
297 8.0–8.5 [42–44]. Desorption of arsenic from goethite may occur by competition  
298 between negative charges for the positive colloid, a reduction of the iron oxide  
299 mineral phase [45], or high pH values ( $>8.5$ ). If plants are present, then the  
300 chemical interactions that take place in the soil–rhizosphere–plant system have to  
301 be considered. According to [46], both plant-induced reductions and drastic pH  
302 decreases in the rhizosphere may dissolve Fe oxides/hydroxides. This would result  
303 in the release of As and the potential uptake by the plant of  $\text{As}^{3+}$  (enhanced  
304 bioavailability and toxicity to plants) [46]. Alternatively, in carbonate-rich rocks  
305 and soils, the acid solutions will become neutral to alkaline, and two arsenic  
306 minerals will precipitate: first weillite ( $\text{Ca}(\text{AsO}_3\text{OH})$ ) and then pharmacolite  
307 ( $\text{CaHAsO}_4 \cdot 2\text{H}_2\text{O}$ ) [33]. Besides, the same authors found remarkable redox sea-  
308 sonal changes for arsenic in river sediments; winter is characterized by a dominance  
309 of  $\text{As}^{3+}$  species within an environment ruled by the activity of bacteria, which leads  
310 to the formation of amorphous  $\text{Fe}^{3+}\text{-As}^{3+}$  precipitates together with nanocrystalline  
311 tooeelite ( $\text{Fe}_6(\text{AsO}_3)_4\text{SO}_4(\text{OH})_4 \cdot 4\text{H}_2\text{O}$ ). On the other hand, biotic oxidation of  
312  $\text{As}^{3+}$  and  $\text{Fe}^{2+}$  leads to the precipitation of mixed  $\text{Fe}^{3+}\text{-As}^{5+}$  hydrous oxides during  
313 spring and summer [33].

### 314 **3 Mining and Pb–Zn Dispersion in Soils: Some Facts** 315 **and Fads**

#### 316 **3.1 How Bad Is the Case?**

317 Mining has indeed a bad press. Poor public relations skills of mining company  
318 officials, the action of environmental groups, and a traditional mistrust from the  
319 ordinary citizens have contributed to create an increasingly poisoned social sce-  
320 nario. There is no question on whether mining strongly polluted the environment

(atmosphere, soils, underground and surface waters, biota, etc.) with heavy metals and/or metalloids prior to the enforcement of environmental regulation laws (from the 1980s onwards) in most countries. However, different to popular beliefs, mining is by no means at present the evil force that many environmental lobbies claim to be. In this regard, if the Earth's land area modified by human action mostly during the last 500 years ( $53.5 \pm 5.1\%$ ) [47] is taken into account, mining and quarrying have contributed with a mere 0.3% (there is a 67% probability that the actual value lies between 0.2% and 0.6%); for comparison, agriculture and forestry contribute with a huge  $46.6 \pm 5.0\%$  [48]. This is particularly significant if it is considered that modern agriculture is the kingdom of chemicals, which are nevertheless a key prerequisite to maintain and even increase global production to sustain an ever-growing human population.

Having said all this, it must be clear on this matter that it is not suggested here that mining (and particularly the smelting of lead minerals) does not pose an important health risk. In fact, lead can affect the nervous system, kidney function, immune system, reproductive and developmental systems, and the cardiovascular system, also affecting the oxygen carrying capacity of the blood; in this regard, this metal is persistent in the environment and accumulates in soils and sediments through deposition from air sources, direct discharge of waste streams to water bodies, mining, and erosion [49]. For example, a comprehensive geochemical and epidemiologic study carried out in 1974 at Coeur d'Alene (Idaho, USA) revealed the following [50]:

- Lead levels in air, soil, and dust were highest at the smelter and decreased with distance, with peak concentrations in soils and vegetation of 9,000 and 3,478 mg kg<sup>-1</sup>, respectively.
- 99% of 1- to 9-year-old children living within 1.6 km from the smelter had blood lead levels  $\geq 40 \mu\text{g dl}^{-1}$ , indicating increased absorption (22% had levels  $\geq 80 \mu\text{g dl}^{-1}$ ).
- Lead levels  $\geq 40 \mu\text{g dl}^{-1}$  decreased with distance, for example, at 72 km from the smelter, it was 1%.
- 17% of children with lead levels of  $\geq 80 \mu\text{g dl}^{-1}$  were anemic.

Another example is related to the Antofagasta (Chile) incident involving lead poisoning in children. Lead was gathered in bulk (Pb mineral concentrates from Bolivia) within the urban zone of the city, which resulted in severe contamination of the surrounding schools and houses. This contamination was in turn significantly associated with high blood lead levels in children [51].

On the other hand, mining and smelting of zinc has been by far the most important contributor of this metal to the environment [26]. For a long time, Zn was not considered to be harmful for the environment, and it was thought to pose minimal health risks compared to other heavy metals; however, at present zinc is known to cause toxic effects in the aquatic biota [26]. Besides, the almost ubiquitous presence of Cd in sphalerite (ZnS) is another factor to be taken into account. Zinc is an essential element, necessary for the function of more than 300 enzymes; however, oral exposure to high levels of zinc in humans can result in several

365 systemic effects [52]. In this regard, the major concerns about Zn are not usually  
366 related to the element but to sphalerite, which usually hosts Cd. This toxic element  
367 causes the so-called itai-itai disease, that is, osteomalacia with various degrees of  
368 osteoporosis accompanied by severe renal tubular diseases [53]. Low-molecular-  
369 weight proteinuria has been reported among people living in contaminated areas in  
370 Japan and exposed to cadmium via food and drinking water [53]. Regarding  
371 arsenic, acute and chronic poisoning involves the respiratory, gastrointestinal,  
372 cardiovascular, nervous, and hematopoietic systems; besides arsenic is carcino-  
373 genic and may cause lung, bladder, liver, renal, and skin cancers [54]. The toxicity  
374 of this metalloid depends on its binding form. For example, the organic arsenic  
375 compounds are less toxic than inorganic species. In fact,  $\text{As}^{3+}$  is 10 times more  
376 toxic than  $\text{As}^{5+}$  and 70 times more toxic than the organic species.

377 Although mining and processing of Pb and Zn in the Iberian Peninsula is  
378 currently restricted to a few mines in the IPB, a myriad of abandoned mines,  
379 tailings, and waste rock dumps are scattered in the old mining districts, and some  
380 of them are in close proximity to towns. For example, Pb–Zn tailings are part of the  
381 urban landscape of Mazarrón [17].

### 382 3.2 When Should We (Really) Worry About?

383 This is an important question that should be addressed from a combined industrial  
384 and environmental perspective including the following factors: mining methods  
385 (underground – open pit); concentration and metallurgical operations; mineralogy  
386 of the ore, gangue, and host rock; fracturing of the host rocks; physiography (hilly  
387 vs. flat terrain); climate; and, last but not least, soil types (pedogenic evolution):

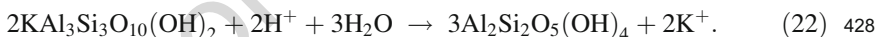
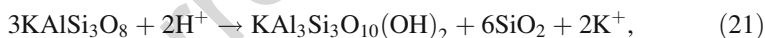
- 388 • *Mining methods*: It does not escape to anyone that the impact of open pit mining  
389 is far larger than the underground procedures. It is a matter of simple mathe-  
390 matics: a usual rate of waste to mineralized rock in open pit operations is 3:1  
391 (or more), meaning that for each ton of rock that will undergo milling and  
392 mineral concentration, three will go into waste; moreover, this three tons will  
393 not be entirely “barren” because they may host subeconomic mineralization  
394 (usually rich in pyrite). In this case, the sulfides present in huge waste rock piles  
395 will be exposed to oxygen and water, which implies generation of AMD and  
396 metal leaching. Besides, once the mining operations have ceased, a huge rock  
397 surface within the pit will be also left to undergo chemical reactions, which may  
398 have disastrous consequences for the chemistry of groundwaters. On the con-  
399 trary, underground mining is more selective (it has to be; otherwise it would turn  
400 out to be uneconomic), and therefore waste rock piling will be minimal. How-  
401 ever, these galleries and stopes placed above the water table may also undergo  
402 oxidation and leaching.
- 403 • *Mineral concentration*: As any other industrial activity, mining has undergone a  
404 complete transformation since the second half of the nineteenth century.

Different to the froth flotation (introduced in the early twentieth century), 405 mineral concentration in the nineteenth century (and well into the twentieth 406 century) was performed by gravity using jigs (e.g., as at Mazarrón and La 407 Unión), an inefficient procedure that contributed to generate tailings deposits 408 extremely rich in Pb and Zn; for example, 4830–21,600 mg kg<sup>-1</sup> Pb and 2410– 409 13,100 mg kg<sup>-1</sup> Zn [17]. 410

- *Mineralogy of the ore, gangue, and host rock:* As previously discussed (1–7), 411 key for the oxidation and leaching of Pb and Zn from galena and sphalerite is the 412 presence of pyrite in the system. Thus, the relative abundance of pyrite among 413 the sulfide species in one particular ore deposit will rule the rate of oxidation 414 during weathering. Other important factors to be taken into account are the fO<sub>2</sub> 415 (no oxygen–no oxidation), water (these are also hydrolytic chemical processes), 416 and biological activity. The latter is driven by the presence of chemolithotrophic 417 bacteria such as (among others) *Thiobacillus ferrooxidans* or *Leptospirillum* spp. 418 [55]. In this regard, the rate of pyrite oxidation directly relates to the rate at 419 which aqueous Fe<sup>3+</sup> can be produced from Fe<sup>2+</sup> by microbial catalysis [56]. In 420 turn, abiotic and biotic oxidation of pyrite generates two powerful chemical 421 leaching agents: sulfuric acid and ferric sulfate (2, 3). However, if the gangue 422 minerals or the host rock includes species such as calcite (CaCO<sub>3</sub>), the acid will 423 react with the carbonate, H<sup>+</sup> will be consumed, and leaching will be reduced or 424 stopped altogether (20): 425



The same applies to the feldspars (21) and their hydrolytic by-products (22) that can 426 be found in volcanic or plutonic rocks [57]: 427



- *Fracturing:* The intensity of fracturing also plays a major role in the oxidation 429 leaching of sulfides. A high density of major fractures facilitates erosion and, 430 therefore, the unroofing of mineral deposits. Once the mineral deposit is in the 431 surface or near surface environment, fracturing will result in increased perme- 432 ability and, therefore, in enhanced movement of oxygen-rich meteoric waters 433 throughout the ore bodies. This implies higher rates of oxidation and metal 434 leaching [57]. 435
- *Climate and physiography:* They do play a major role in metal dispersion. Given 436 that leaching of metals is an essentially chemical process, temperature will play 437 a crucial role: warmer conditions will enhance the process, whereas cold condi- 438 tions will slow it down. Total rain precipitation is also important [17]. 439 For example, rainfall and dry events cause increases and decreases, respectively, 440 in acid and metal concentrations. The process does not end until pyrite is fully 441 weathered, which can take hundreds to thousands of years [58]. As noted by 442

443 [58], long dry spells result in gradual increases in metal concentrations, whereas  
444 sudden large increases are observed during initiation of rains. However, as  
445 precipitations reach their peak, the solutions become diluted. On top of this,  
446 the flash floods generated during stormy episodes must be added as they have the  
447 capacity to remove contaminated soils and tailings deposits. If this occurs,  
448 massive transport of contaminated materials will go to the rivers and, from  
449 there, to the lowlands. This is a process that will be enhanced by the high-  
450 altitude environment. In this regard, the rule of thumb is: the higher a mining  
451 operation is located, the greater the risk of mass movement of contaminated  
452 materials. This is well exemplified by cases in Chile (Pascua – Lama, El Indio  
453 Belt) and New Guinea (OK Tedi, Grasberg, Porgera) (e.g., [2, 40, 57], of this  
454 chapter).

455 • *Soil types (pedogenic evolution)*: The retention and accumulation of metals in  
456 the soil depends on various soil characteristics such as solid phase components  
457 (organic matter, sulfates, carbonates and clay minerals, oxides, etc.), texture,  
458 structure, pH, and ion exchange capacity (e.g., [13, 17]). These soil character-  
459 istics are intimately related to the climate and physiography in terms of soil  
460 evolution. Organic matter plays a key role as they may form very stable organic-  
461 mineral complexes and they have a very high ion exchange capacity. Alterna-  
462 tively, soluble humic substances as fulvic acids may form quelates that facilitate  
463 the metal leaching from the soil. Soil mineralogy is crucial because of the  
464 importance of adsorption processes and ion exchange capacity in clays and  
465 oxides, hydroxides, and oxyhydroxides and metal coprecipitation in sulfates  
466 and carbonates. The presence of soluble salts may affect the pH and the ion  
467 (cation) exchange of metals. Texture and structure control the water–rock  
468 interaction and solid phase reactivity through specific surface and hydraulic  
469 conductivity. The pH in terms of active and potential acidity plays a dual role,  
470 firstly because it controls the ion exchange capacity (especially in organic  
471 matter) and secondly because metal solubility depends on pH.

472 These reasons explain why risk assessment of metal leaching from ore deposits,  
473 tailings, and waste rock dumps is so complex. In fact, it involves complex nonlinear  
474 systems in which the measurements of the pollutant phase(s) (and other variables:  
475 see above) alone cannot provide a complete picture of the state of the system,  
476 because they are limited in space and time. However, at least a partial answer may  
477 be provided to the initial question on when we should be worried regarding metal  
478 leaching. In this process nothing is as decisive as: (1) the proportion of pyrite in the  
479 sulfide mineral assemblage and (2) the reactivity of the gangue and host rock  
480 minerals. This puts the IPB deposits in the worst possible case scenario (extremely  
481 rich in pyrite).



## 4 Pb, Zn, Cd, and As in Soils from the Studied Iberian Mining Sites and Districts 482 483

To study the Pb, Zn, Cd, and As distribution in soils from the revised mining sites 484 and districts (Fig. 1, Table 1), published data from soils subjected to different uses 485 (agricultural, natural, and anthropic) have been considered (Table 2). The more 486 polluted soils were identified on the basis of a relative enrichment factor ( $REF_{\text{metal}}$ ), 487 defined by the ratio  $([\text{metal concentration in polluted soil} - \text{metal background concentration in soil}] / [\text{metal background concentration in soil}])$ . By using the 488  $REF$  value, it is assumed that soils may have high background metal concentrations 489 in natural, nonpolluted conditions as they are in areas that host ore deposits. Indeed, 490 ore deposits induce the generation of geochemical dispersion halos, which can be 491 regarded as a “natural contamination process” different to these of industrial origin 492 generated by mining, processing, and smelting of sulfide ores. The relationships 493 between metals and As (arsenic is a metalloid) were studied by correlation matrices, 494 and cluster and factor analyses were also used to investigate whether different 495 geological and industrial scenarios resulted in the formation of differentiated 496 clusters of mineral deposits. Below detection limit (BDL) data were set to a value 497 of half the BDL concentration for each element [59]. Besides, given that a sizeable 498 proportion of data with identical value can seriously influence any multivariate 499 analysis [4, 60], the sets with BDL data  $>10\%$  of the population were excluded. 500 [\[AU6\]](#)

Log transformation was applied to data to get more symmetrical (Gaussian) distri- 502 butions. In this regard, many trace element distributions show important skewness, 503 which may disappear if the logarithm of the values ( $\log x$ ) is considered. If this is 504 the case, it can be said that  $\log x$  has a normal distribution, or simpler, that the 505 distribution is lognormal [61]. 506

Although there are significant differences in size among the data sets, the 507 following facts can be highlighted in terms of mean concentrations and enrichment 508 factors. 509

### 4.1 Mean Concentrations 510

- The highest Pb and Zn mean concentrations are found in soils located in the 511 Sierra Minera (La Unión District) with values of 6,241 and 9,111  $\text{mg kg}^{-1}$ , 512 respectively (Fig. 2, Table 2). However, the data population shows a large 513 dispersion with some outliers of very high concentrations that displace the 514 mean outside the first quartile (Q1) and third quartile (Q3) range (Fig. 2, Table 2). 515 The lowest Pb and Zn mean concentrations are found in soils located in 516 Rodalquilar (226.3 and 118.9  $\text{mg kg}^{-1}$ , respectively) (Fig. 2, Table 2). 517
- The highest As mean concentration (1,309  $\text{mg kg}^{-1}$ ) is also found in soils from 518 the Sierra Minera (Fig. 2, Table 2), whereas the lowest As mean concentration 519 (26.1  $\text{mg kg}^{-1}$ ) is found in Linares (Fig. 2, Table 2). 520

t.1 **Table 2** Descriptive basic statistics of trace element concentrations. Mean, median, minimum, maximum, first quartile (Q1), and third quartile (Q3) values are expressed in mg kg<sup>-1</sup>

t.2	Variable (n = 126)	Analysis method	Mean	St. Dev.	Min.	Q1	Median	Q3	Max.
t.3	<i>Linares (Source: [8])</i>								
t.4	Ag	ICP-AES	2.1	4.3	0.3	0.3	0.5	1.8	29.2
t.5	As	ICP-AES	26.1	29.2	2.5	11	17	26	175.5
t.6	Cd	ICP-AES	0.8	2.9	0.2	0.2	0.2	0.6	31.8
t.7	Cu	ICP-AES	145.4	242.5	14	32.8	53.5	128.4	1,654
t.8	Pb	ICP-AES	4077	7,016	27	267	1,279	4,867	37,356
t.9	Sb	ICP-AES	18.6	90	2.5	2.5	2.5	10	992
t.10	Zn	ICP-AES	123.9	206	26	46	71.5	133.5	1,988
t.11	Mn	ICP-AES	1,210.7	802.1	194	530.8	1,086	1,608	3,981
t.12	<i>Valdequilar (n = 31) (Source: [24])</i>								
t.13	<i>Rodulquilar (Source: [24])</i>								
t.14	As	ICP-MS	422	473.1	27.4	70.4	169	784	1,510
t.15	Bi	ICP-MS	8.5	13.9	0	1	2.8	10.2	73.5
t.16	Cd	ICP-MS	0.3	0.2	0.1	0.1	0.2	0.2	0.8
t.17	Cu	ICP-MS	73.6	49.5	11.2	39.8	57.5	102	178
t.18	Hg	Pyrolysis	0.4	0.6	0	0.1	0.2	0.5	2.6
t.19	Pb	ICP-MS	226.3	158.7	28.2	115	193	270	798
t.20	Sb	ICP-MS	19.4	18.8	0.6	4.6	10.7	32.2	62.6
t.21	Se	ICP-MS	15.7	14.5	1.5	3.9	8.9	27.5	49.8
t.22	Sn	ICP-MS	25.7	28.5	2	5	11	37	108
t.23	Zn	ICP-MS	118.9	103.3	1.3	42.4	77.2	160	401
t.24	<i>Valdequilar (n = 15) (Source: [17])</i>								
t.25	<i>Mazarrón (Source: [17])</i>								
t.26	Ag	ICP-MS	9.7	11.2	0.4	2.5	6.4	12.4	36
t.27	As	ICP-MS	252.3	206.6	58	98	189	299	744
t.28	Ba	ICP-MS	1,212	1,425	149	485	774	1,390	6,050
t.29	Bi	ICP-MS	0.3	0.6	0.01	0.1	0.2	0.4	2.4
t.30	Cd	ICP-MS	11.4	9.9	0.7	5	7.6	18	32.8
t.31	Cu	ICP-MS	88.7	59.4	27	41	80	123	259
t.32	Pb	ICP-MS	2,955	2,570	235	908	2,600	4,820	9,110
t.33	Sb	ICP-MS	54.4	42.2	10.3	27.3	40.5	80.1	174
t.34	Se	ICP-MS	1.2	0.4	0.5	1.1	1.2	1.4	2
t.35	Sn	ICP-MS	14.3	10.6	4	9	11	14	48
t.36	Zn	ICP-MS	1,651	1,584	331	563	791	3,030	5,250
t.37	<i>Valdequilar (n = 54) (Source: [22])</i>								
t.38	<i>Sierra Minera (Source: [22])</i>								
t.39	As	AFS	1,309	1,123	67	453	1,020	1,597	4,429
t.40	Cd	ETAAS	37.6	22.6	2.2	22.2	33.7	44.5	123.2
t.41	Cu	ETAAS	352.1	293.4	21.5	140.5	258.4	576.2	1,335
t.42	Hg	AFS	0.3	0.5	0	0	0.1	0.4	2
t.43	Pb	ETAAS	6,241	9,390	25	2,287	3,328	4,222	47,619
t.44	Zn	FAAS	9,111	6,911	516	3,223	7,844	11,336	30,405

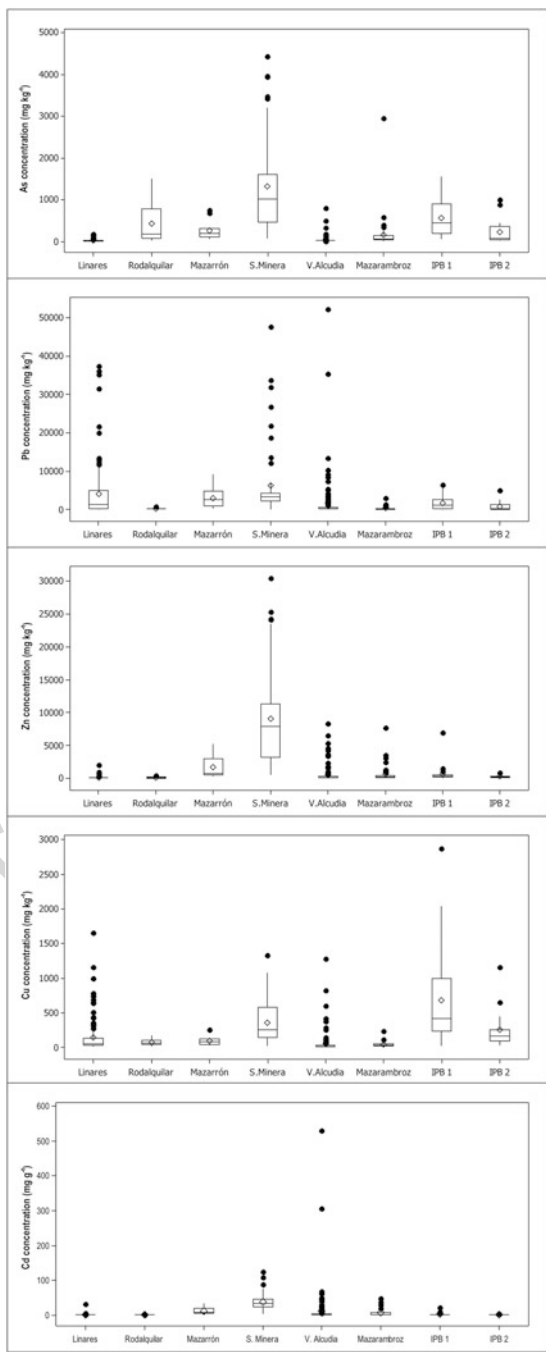
(continued)

**Table 2** (continued)

Variable ( <i>n</i> ≠ 126)	Analysis method	Mean	St. Dev.	Min.	Q1	Median	Q3	Max.	t.45
Variable ( <i>n</i> = 142)									
<i>Alcudia</i> (Source: [2])									
As	EDXRF	37.4	83.16	0.5	17	22	26	792	t.49
Cd	EDXRF	10.53	51.83	0.5	0.5	0.5	2	530	t.50
Cr	EDXRF	33.84	33.39	0.5	14	26	44.25	253	t.51
Cu	EDXRF	56.6	150	1	11	15.5	31	1,283	t.52
Hg	EDXRF	71.4	342.7	0.5	0.5	0.5	0.5	2,665	t.53
Mo	EDXRF	3.067	3.702	0.5	0.5	1	5	19	t.54
Ni	EDXRF	12.3	21.63	0.5	0.5	4.5	16	137	t.55
Pb	EDXRF	1,575	5,581	69	112	169	544	52,207	t.56
Sb	EDXRF	2.98	12.37	0.5	0.5	0.5	0.5	110	t.57
Se	EDXRF	33.7	27.56	18	25	27	31	282	t.58
Zn	EDXRF	517	1,232	30	61	112	259	8,336	t.59
Variable ( <i>n</i> = 50)									
<i>Mazarambroz</i> (Source: [16])									
As	EDXRF	161.8	417.5	11	30	61	140.5	2,955	t.62
Cd	EDXRF	5.69	10.02	0.5	0.5	0.5	7.25	47	t.63
Cr	EDXRF	52.11	45.45	0.5	21.75	46	75	244	t.64
Cu	EDXRF	40.78	36.22	8	17.75	32.5	50.5	232	t.65
Hg	EDXRF	0.5	0	0.5	0.5	0.5	0.5	0.5	t.66
Mo	EDXRF	9.84	3.285	3	8	10	12	19	t.67
Ni	EDXRF	22.3	23.49	0.5	6	18	29	112	t.68
Pb	EDXRF	307.9	472.8	86	97	109.5	267.3	2,867	t.69
Sb	EDXRF	0.73	1.626	0.5	0.5	0.5	0.5	12	t.70
Se	EDXRF	22.64	6.444	0.5	21	24	26	32	t.71
Zn	EDXRF	603	1,251	67	110	160	389	762	t.72
Variable ( <i>n</i> = 32)									
<i>IPB1</i> (Source: [12])									
As	INAA	562.4	441.9	51	185.5	443.5	896	1,560	t.75
Cd	ICP-AES	1.744	3.99	0.15	0.15	0.65	1	22	t.76
Cr	INAA	77.84	51.34	2.5	48.25	73	94.25	226	t.77
Cu	ICP-AES	684	678	24	238	413	992	2,874	t.78
Hg	INAA	6.78	14.5	0.5	0.5	0.5	4.75	62	t.79
Ni	ICP-AES	34.69	29.93	0.5	12	30.5	51.75	138	t.80
Pb	ICP-AES	1,705	1,839	59	239	1,165	2,637	6,500	t.81
Zn	ICP-AES	599	1,192	22	175	354	500	6,890	t.82
Variable ( <i>n</i> = 15)									
<i>IPB2</i> (Source: [11])									
As	INAA	226.8	315.8	18.8	30.2	78.7	361	994	t.84
Cd	ICP-AES	0.917	0.529	0.15	0.5	0.8	1.2	2.3	t.86
Cr	INAA	129.3	56.8	35	98	111	173	236	t.87
Cu	ICP-AES	259.7	296.8	27	90	159	253	1,160	t.88
Ni	ICP-AES	45.93	20.23	14	26	51	60	75	t.89
Pb	ICP-AES	810	1,341	41	93	197	1,270	4,890	t.90
Zn	ICP-AES	303.1	233.9	95	147	206	356	897	t.91

ICP-AES, inductively coupled plasma atomic emission spectroscopy; ICP-MS, inductively coupled plasma mass spectrometry; AFS, atomic fluorescence spectroscopy; FAAS, flame atomic absorption spectrometry; ETAAS, electrothermal atomization atomic absorption spectrometry; EDXRF, energy dispersive X-ray fluorescence; INAA, instrumental neutron activation analysis

**Fig. 2** Box-and-whisker plot for As, Pb, Zn, Cu, and Cd concentrations. The central box covers the middle half of the data, extending from the lower (Q1) to the upper quartile (Q3). The lines extending above and below the box (*whiskers*) show the range from which the not included data are considered as outsiders. The median of the data is indicated by the *horizontal line* within the box, whereas the *diamond sign* shows the location of the arithmetic mean



- The highest Cd mean concentration ( $37.6 \text{ mg kg}^{-1}$ ) is also from the Sierra Minera (Fig. 2, Table 2), whereas the lowest is found in Rodalquilar ( $0.2 \text{ mg kg}^{-1}$ ) (Fig. 2, Table 2).

#### 4.2 Enrichment Factors (*REF<sub>metal</sub>*)

524

- The most Pb–Zn polluted soils correspond to those of the Sierra Minera (Fig. 3, Table 3) with Pb and Zn at more than 488 and 163 times the background, respectively. Conversely, the least Pb–Zn polluted soils are those of Linares, with Pb at 2.5 times the background value and Zn close to the background.
- The most As polluted soils are those of the Sierra Minera (Fig. 3, Table 3) at ~98 times the background value. On the other hand, the less polluted soils correspond to those located in Linares (Fig. 3, Table 3) at less than 0.5 times the background value.
- The most Cd polluted soils are found in the Sierra Minera (Fig. 3, Table 3) at more than 99 times the background value, whereas the less polluted soils are those from IPB, close to the background values.

#### 4.3 Correlations and Clustering of Data

536

- The highest correlations in soils from the Alcudiva Valley are found for the Pb–Zn and Pb–Cu pairs (0.86), whereas insignificant correlations are found for As–Zn and As–Cr (0.02 and 0.07, respectively) (Table 4). Thus, the lack of relation among As and metals is remarkable (Fig. 4).
- Contrary to the results for the Alcudiva Valley, the strongest correlation in the (IPB) is found for the As–Pb pair (0.80 in the data set IPB1 and 0.91 in data set IPB2) (Table 4). In this regard, As gets clustered with Pb and Cu in the two populations, whereas Zn appears to show more affinity for Cd and Cr with Ni (Fig. 4).
- The strongest correlation in Linares is found for the pair As–Pb (0.81) (Table 4), which is also indicated by the cluster analysis (Fig. 4). Besides, the lowest correlation is shown by the Pb–Zn and Cu–Zn pairs (0.65) (Table 4), a fact also shown by the cluster analysis (Fig. 4).
- The data from Mazarrón show a pattern similar on that observed for the IPB data sets, with As clustering with Pb and Cu (and also Ag in the Mazarrón case) (Fig. 4). Zn clusters with Cd, whereas Cr does it with Ni. The As–Pb is well correlated (0.81) (Table 4) although the highest correlation corresponds to the Ag–Pb pair (0.94) (Table 4). The pairs Ba–Cu and Ba–Sn display the lowest correlations ( $-0.06$  and  $0$ , respectively) (Table 4).
- The strongest correlation in the data from Sierra Minera is shown by the As–Cu pair (0.70) (Table 4), and the lowest corresponds to the As–Hg pair ( $-0.01$ ) (Table 4).

**Fig. 3** Box-and-whisker plot for As, Pb, Zn, Cu, and Cd relative enrichment factors ( $REF_{\text{metal}} = [\text{metal concentration in polluted soil} - \text{metal background concentration in soil}] / [\text{metal background concentration in soil}]$ ). Explanation as in Fig. 2

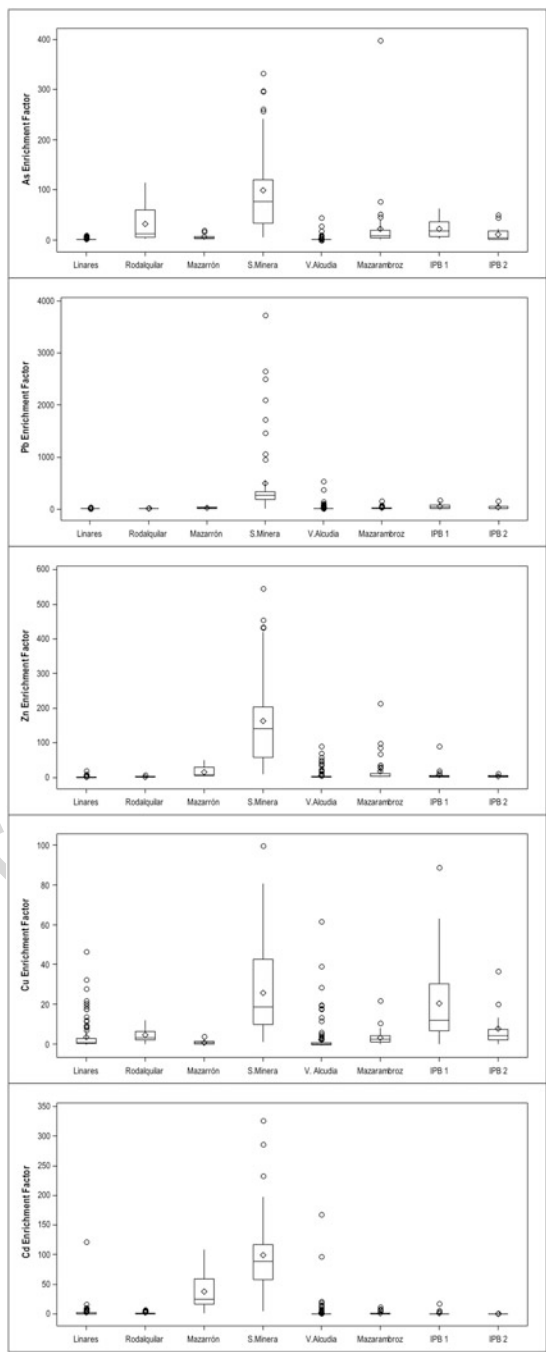


**Table 3** Descriptive basic statistics of relative enrichment factors (REF<sub>metal</sub>) of As, Pb, Zn, Cu, and Cd. Mean, median, minimum, maximum, first quartile (Q1), and third quartile (Q3) values are expressed in per unit of the background value

District	Backgrd	Source	N	Mean	St. Dev.	Min.	Q1	Median	Q3	Max.
<i>As</i>										
Linares	18.09	[7, 8]	126	0.4	1.6	-0.9	-0.4	-0.1	0.4	8.8
Rodalquilar	13.15	[24]	31	31.1	36	1.1	4.4	11.9	58.6	113.8
Mazarrón	39.33	[17]	15	5.4	5.3	0.5	1.5	3.8	6.6	17.9
S. Minera	13.25	[22]	54	97.8	84.8	4.1	33.2	76	119.6	333.2
V. Alcudia	17.5	[2]	142	1.1	4.8	-1	0	0.3	0.5	44.3
Mazarambroz	7.4	[62]	50	20.9	56.4	0.5	3.1	7.2	18	398.3
IPB1	25	[63]	32	21.5	17.7	1	6.4	16.7	34.8	61.4
IPB2	20	[11]	15	10.3	15.8	-0.1	0.5	2.9	17.1	48.7
<i>Pb</i>										
Linares	1,212	[7, 8]	126	2.4	5.8	-1	-0.8	0.1	3	29.8
Rodalquilar	33	[24]	31	5.9	4.8	-0.1	2.5	4.8	7.2	23.2
Mazarrón	159.67	[17]	15	17.5	16.1	0.5	4.7	15.3	29.2	56.1
S. Minera	12.75	[22]	54	488	736	1	178	260	330	3,734
V. Alcudia	96.9	[2]	142	15.3	57.6	-0.3	0.2	0.7	4.6	537.8
Mazarambroz	19.3	[62]	50	15	24.5	3.5	4	4.7	12.9	147.6
IPB1	38	[63]	32	43.9	48.4	0.6	5.3	29.7	68.4	170.1
IPB2	31	[11]	15	25.1	43.3	0.3	2	5.4	40	156.7
<i>Zn</i>										
Linares	100.79	[7, 8]	126	0.2	2	-0.7	-0.5	-0.3	0.3	18.7
Rodalquilar	54	[24]	31	1.2	1.9	-1	-0.2	0.4	2	6.4
Mazarrón	103.67	[17]	15	14.9	15.3	2.2	4.4	6.6	28.2	49.6
S. Minera	55.5	[22]	54	163.2	124.5	8.3	57.1	140.3	203.2	546.8
V. Alcudia	92	[2]	142	4.6	13.4	-0.7	-0.3	0.2	1.8	89.6
Mazarambroz	35.7	[62]	50	15.9	35	0.9	2.1	3.5	9.9	212.6
IPB1	76	[63]	32	6.9	15.7	-0.7	1.3	3.7	5.6	89.7
IPB2	72	[11]	15	3.2	3.2	0.3	1	1.9	3.9	11.5
<i>Cu</i>										
Linares	34.82	[7, 8]	126	3.2	7	-0.6	-0.1	0.5	2.7	46.5
Rodalquilar	14.1	[24]	31	4.2	3.5	-0.2	1.8	3.1	6.2	11.6
Mazarrón	55.33	[17]	15	0.6	1.1	-0.5	-0.3	0.4	1.2	3.7
S. Minera	13.25	[22]	54	25.6	22.1	0.6	9.6	18.5	42.5	99.8
V. Alcudia	20.5	[2]	142	1.8	7.3	-1	-0.5	-0.2	0.5	61.6
Mazarambroz	10.3	[62]	50	3	3.5	-0.2	0.7	2.2	3.9	21.5
IPB1	32	[63]	32	20.4	21.2	-0.3	6.4	11.9	30	88.8
IPB2	31	[11]	15	7.4	9.6	-0.1	1.9	4.1	7.2	36.4
<i>Cd</i>										
Linares	0.26	[7, 8]	126	2	11	-0.2	-0.2	-0.2	1.4	121.3
Rodalquilar	0.1	[24]	31	1.5	2.1	0	0	1	1	7
Mazarrón	0.3	[17]	15	37.1	33.1	1.3	15.7	24.3	59	108.3
S. Minera	0.38	[22]	54	99.2	60.3	4.8	58.3	88.9	117.5	327.4
V. Alcudia	3.14	[2]	142	2.4	16.5	-0.8	-0.8	-0.8	-0.4	168.1
Mazarambroz	3.9	[62]	50	0.5	2.6	-0.9	-0.9	-0.9	0.9	11.1
IPB1	1.2	[12]	32	0.5	3.3	-0.9	-0.9	-0.5	0.1	17.2
IPB2	1.2	[12]	15	-0.2	0.4	-0.9	-0.6	-0.3	0	0.9

Sources of the background concentrations used in this chapter are indicated in the Backgrd column. *Backgrd* background, *St. Dev.* standard deviation, *Min.* minimum, *Max.* maximum

t.1 **Table 4** Correlation index matrices for element concentrations (log10) from all data sets. For the correlation analysis, metal sets with more than 10% of all values of BDL data have been excluded from the original data sets (Linares Ag, Cd, Sb; Rodalquilar Cd; Mazarrón Bi; Alcudia Cd, Hg, Mo, Ni, S; Mazarambroz Cd, Cr, Hg, Ni, Sb; IPB1 Hg)

t.2	As	Cu	Pb							
t.3	<i>Linares</i>									
t.4	Cu	0.76								
t.5	Pb	0.81	0.78							
t.6	Zn		0.65	0.65						
t.7	Ag		Bi	Cu	Hg	Pb	Sb	Se	Sn	
t.8	<i>Rodalquilar</i>									
t.9	Bi	0.82								
t.10	Cu	0.62	0.7							
t.11	Hg	0.26	0.33	0.2						
t.12	Pb	0.42	0.46	0.72	0.21					
t.13	Sb	0.87	0.71	0.58	0.27	0.28				
t.14	Se	0.91	0.71	0.46	0.4	0.22	0.87			
t.15	Sn	0.95	0.85	0.57	0.29	0.34	0.86	0.91		
t.16	Zn		0.33	0.58	-0.16	0.65	0.29	0.26	0.35	
t.17	Ag	As	Ba	Cd	Cu	Pb	Sb	Se	Sn	
t.18	<i>Mazarrón</i>									
t.19	As	0.89								
t.20	Ba	0.17	0.29							
t.21	Cd	0.18	0.23	0.30						
t.22	Cu	0.66	0.77	-0.06	0.55					
t.23	Pb	0.94	0.81	0.14	0.37	0.74				
t.24	Sb	0.51	0.58	0.83	0.41	0.21	0.50			
t.25	Se	0.13	0.23	0.45	0.19	0.09	0.12	0.46		
t.26	Sn	0.42	0.42	0.00	0.60	0.53	0.55	0.42	0.52	
t.27	Zn		0.30	0.37	0.73	0.48	0.58	0.54	0.37	0.63
t.28	Ag	Cd	Cu	Fe	Hg	Pb				
t.29	<i>Sierra Minera</i>									
t.30	Cd	0.25								
t.31	Cu	0.70	0.31							
t.32	Fe	0.57	0.50	0.55						
t.33	Hg	-0.01	0.18	0.23	0.14					
t.34	Pb	0.61	0.42	0.58	0.68	0.21				
t.35	Zn		0.46	0.56	0.42	0.31	0.43			
t.36	Ag	Cr	Cu	Pb	Se					
t.37	<i>Alcudia Valley</i>									
t.38	Cr	0.07								
t.39	Cu	0.15	0.22							
t.40	Pb	0.14	0.21	0.86						
t.41	Se	0.23	0.25	0.79	0.84					
t.42	Zn	0.02	0.17	0.86	0.86	0.68				

(continued)



**Table 4** (Continued)

	As	Cu	Pb			
	As	Cu	Mo	Pb	Se	
<i>Mazarambroz</i>						
Cu	0.64					
Mo	0.01	0.18				
Pb	0.56	0.49	0.27			
Se	-0.65	-0.3	0.09	-0.27		
Zn		0.62	0.33	0.89	-0.24	
		Cd	Cr	Cu	Ni	Pb
<i>IPB1</i>						
Cd	0.16					
Cr	0.06	0.09				
Cu	0.42	0.47	0.19			
Ni	0.25	0.27	0.71	0.49		
Pb	0.80	0.29	0.16	0.71	0.43	
Zn	0.25	0.68	-0.02	0.65	0.45	0.51
<i>IPB2</i>						
Cd	0.53	1.00				
Cr	0.16	-0.30	1.00			
Cu	0.90	0.55	0.13	1.00		
Ni	0.64	0.44	0.49	0.67	1.00	
Pb	0.91	0.57	0.00	0.87	0.46	1.00
Zn	0.80	0.61	-0.20	0.69	0.33	0.91

(Table 4). The cluster analysis allows the observation of some patterns reflecting the moderate correlation indexes among As, Cu, Pb, Zn, and Cd pairs and the low affinity of Hg with the other metals and As (Fig. 4).

- The strongest correlation in Rodalquilar is found for the pair As–Sn (0.95) (Table 4), with As being weakly related to the Pb–Zn–Cu group (Fig. 4).
- The strongest correlation from the Mazarambroz soils occurs in the Pb–Zn pair (0.89) (Table 4), whereas the most weak corresponds to the As–Mo pair (0.02) (Table 4). The cluster analysis of the Mazarambroz data is consistent with the correlation matrix, showing the Pb–Zn and As–Cu affinities (Fig. 4).

## 5 Conclusions

From the above results, some conclusions may be attained. The clustering of As and metals allows identification of several pollution modes, which in turn may correspond to significant differences in metal partitioning and solid phase bounding:

- The As–Pb–(Cu) + Zn–Cd mode that can be regarded as representative of the IPB, Linares, and Mazarrón. This suggests that the metals of each pair are similarly partitioned into the soil and bound to the same mineral phases, for

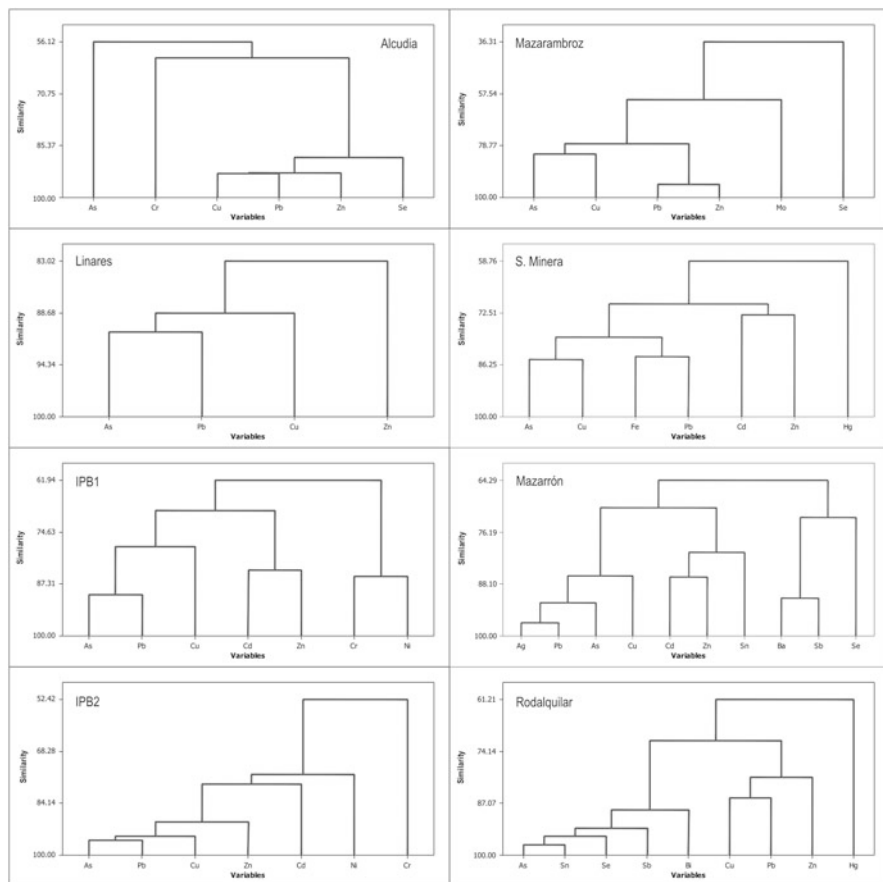


**Fig. 4** Dendrogram (clusters by group average) for all data sets. Data are log-transformed, and metal sets with more than 10% of all values of BDL data have been excluded for the cluster analysis (Linares Ag, Cd, Sb; Rodalquilar Cd; Mazarrón Bi; Alcudia Cd, Hg, Mo, Ni, Sb; Mazarambroz Cd, Cr, Hg, Ni, Sb; IPB1 Hg)

574 example, As and Pb to iron oxyhydroxides ([12, 17]); alternatively, [11] and [13]  
 575 have suggested that As, Pb, and Zn are mainly bound to Fe and Mn oxides with  
 576 some Pb and Zn associated with the exchangeable fraction consisting of  
 577 phyllosilicates and carbonates.

- 578 • The As–Cu mode that may be regarded as representative of: (a) the Sierra  
 579 Minera with As–Cu + Pb–Zn + Cd–Zn pattern and (b) Mazarambroz with a Pb–  
 580 Zn + As–Cu pattern. The As–Cu pair appears to be related to jarosite in the Sierra  
 581 Minera [22]. At Mazarambroz Pb seems to be bound to supergenic carbonates  
 582 and sulfates, whereas As would be bound to iron oxyhydroxides [16].
- 583 • The As–Sn + Cu–Pb–(Zn) mode is observed at Rodalquilar where Pb is bound to  
 584 Mn oxide phases and As is bound to goethite [24].

- The Cu–Pb–Zn mode with As showing a weak affinity for those metals as observed at the Alcudiva Valley. In the San Quintín mines, most of Pb is bound to reducible forms (Fe and Mn oxides), whereas Zn occurs mainly as an exchangeable, water- and acid-soluble form (e.g., carbonates; [4]).

A second conclusion is that these modes do not necessarily relate to the intensity of pollution in terms of absolute concentrations of metals or  $REF_{\text{metal}}$ . For example, the most As–Pb–Cd polluted district (Sierra Minera) does not show the same pattern as the IPB, Rodalquilar, or Mazarrón (Fig. 2, 3) (Tables 2, 3).

A third conclusion relates to the fact that the As–metal affinities seem to be controlled by other factors than exclusively mineral paragenesis and/or pyrite abundance. For example, Linares (a district where the ore deposits are characterized by low contents of pyrite and an important presence of carbonates that preclude a significant AMD production, [64]) displays nevertheless a similar (As–Pb–(Cu)) pattern to that of the IPB, the most representative district of AMD in the Iberian peninsula (e.g., [65]) and of the worst cases worldwide. On the other hand, the distinct pattern of metal clustering in some districts could be related to the mineral paragenesis as seen in Rodalquilar where the alteration type and minerals associated to the high-sulfidation ore-forming processes ultimately played a key role in the As and metal fate in soils (Table 1, [24]).

A fourth conclusion is that some of the most As–Pb–Zn–Cd polluted districts in terms of  $REF_{\text{metal}}$  (Sierra Minera, Rodalquilar, IPB, and Mazarrón) have a semiarid Mediterranean climate, characterized by a high evapotranspiration during the dry and hot summer. That process induces the ascent of metal-rich water in the soil by capillarity and the subsequent metal enrichment in the top soil, mostly in the form of soluble phases as sulfates and carbonates [66], which in turn will be dissolved during heavy rain stormy episodes. Thus, these rain events can produce high rates of metal leaching and mobilization by runoff (e.g., [17, 22]).

**Acknowledgments** The study presented in this chapter was partly funded by the Spanish Ministry of Economy and Competitiveness (Project CTM2012-33918).

## References

1. Palero FJ, Both RA, Arribas A, Boyce AJ, Mangas J, Martín-Izard A (2003) Geology and metallogenic evolution of the polymetallic deposits of the Alcudiva Valley Mineral Field, eastern Sierra Morena, Spain. *Econ Geol* 98:577–605
2. Higuera P, Oyarzun R, Iraizoz JM, Lorenzo S, Esbrí JM, Martínez Coronado A (2014) Low-cost geochemical surveys for environmental studies in developing countries: testing a field portable XRF instrument under quasi-realistic conditions. *J Geochem Explor* 113:3–12
3. Oyarzun R, Fernández Barrenechea J, Esbrí JM, Higuera P, Lillo J, Martínez Coronado A, López García JA, López Andrés S (2010) *Geoquímica Ambiental en San Quintín*. Grupo Minero San Quintín (Ciudad Real): Sitio docente de entrenamiento activo para evaluaciones ambientales (Environmental Geochemistry in San Quintín. San Quintín Mining Group, Ciudad

- 625 Real: learning site for training in environmental assessments). [http://www.aulados.net/](http://www.aulados.net/GEMM/Documentos/San_Quintin_Innova/index.html)  
626 [GEMM/Documentos/San\\_Quintin\\_Innova/index.html](http://www.aulados.net/GEMM/Documentos/San_Quintin_Innova/index.html). Accessed 12 Jun 2014
- 627 4. Rodríguez L, Ruiz E, Alonso-Azcárate J, Rincón J (2009) Heavy metal distribution and  
628 chemical speciation in tailings and soils around a Pb-Zn mine in Spain. *J Environ Manage*  
629 90:1106–1116
- 630 5. Lillo J (2002) Hydrothermal alteration in the Linares-La Carolina Ba-Pb-Zn-Cu-(Ag) vein  
631 district, Spain: mineralogical data from El Cobre vein. *T I Min Metall B* 111:114–118
- 632 6. Martínez J, Llamas JF, De Miguel E, Rey J, Hidalgo MC (2008) Soil contamination from urban  
633 and industrial activity: example of the mining district of Linares (southern Spain). *Environ*  
634 *Geol* 54:669–677
- 635 7. Martínez J, Llamas J, De Miguel E, Rey J, Hidalgo MC (2007) Determination of geochemical  
636 back ground in a metal mining site: example of the mining district of Linares (south Spain).  
637 *J Geochem Explor* 94:19–29
- 638 8. Martínez López J, Llamas Borrajo J, De Miguel GE, Rey Arrans J, Hidalgo Estévez MC, Sáez  
639 Castillo AJ (2008) Multivariate analysis of contamination in the mining district of Linares  
640 (Jaén, Spain). *Appl Geochem* 23:2324–2336
- 641 9. Leistel JM, Marcoux E, Thiéblemont D, Quesada C, Sánchez A, Almodovar GR, Pascual E,  
642 Sáez R (1998) The volcanic-hosted massive sulphide deposits of the Iberian Pyrite Belt. *Miner*  
643 *Deposita* 33:2–30
- 644 10. Chopin EIB, Alloway BJ (2007) Trace element partitioning and soil particle characterisation  
645 around mining and smelting areas at Tharsis, Riotinto and Huelva, SW Spain. *Sci Total*  
646 *Environ* 373:488–500
- 647 11. López M, González I, Romero A (2008) Trace elements contamination of agricultural soils  
648 affected by sulphide exploitation (Iberian Pyrite Belt, SW Spain). *Environ Geol* 54:805–818
- 649 12. Fernández-Caliani JC, Barba-Brioso C, González I, Galán E (2009) Heavy metal pollution in  
650 soils around the abandoned mine sites of the Iberian Pyrite Belt (Southwest Spain). *Water Air*  
651 *Soil Poll* 200:211–226
- 652 13. González I, Galán E, Romero A (2011) Assessing soil quality in areas affected by sulfide  
653 mining. Application to soils in the Iberian Pyrite Belt (SW Spain). *Minerals* 1:73–108
- 654 14. Villaseca C, López-García JA, Barbero L (2005) Estudio de la composición isotópica (Pb-S-O)  
655 de las mineralizaciones Pb–Zn de Mazarambroz (Banda Milonítica de Toledo) (Study of the  
656 isotopic composition (Pb-S-O) of the Mazarambroz (Toledo Mylonitic Band) mineralization).  
657 *Geogaceta* 38:271–274
- 658 15. López-García JA, Villaseca C, Barbero L (2003) Estudio preliminar de las mineralizaciones de  
659 Pb-Zn de Mazarambroz, Banda Milonítica de Toledo (Preliminary study of the Pb-Zn miner-  
660 alization in Mazarambroz (Toledo Mylonitic Band)). *Boletín de la Sociedad Española de*  
661 *Mineralogía* 26-A:171–172
- 662 16. González-Corrochano B, Esbrí JM, Alonso-Azcárate J, Martínez-Coronado A, Jurado V,  
663 Higuera P (2014) Environmental geochemistry of a highly polluted area: the La Union  
664 Pb-Zn mine (Castilla-La Mancha region, Spain). *Dig J Geochem Explor*. doi:10.1016/j.  
665 [gexplo.2014.02.014](https://doi.org/10.1016/j.gexplo.2014.02.014)
- 666 17. Oyarzun R, Lillo J, López-García JA, Esbrí JM, Cubas P, Llanos W, Higuera P (2011) The  
667 Mazarrón Pb-(Ag)-Zn mining district (SE Spain) as a source of heavy metal contamination in a  
668 semiarid realm: Geochemical data from mine wastes, soils, and stream sediments. *J Geochem*  
669 *Explor* 109:113–124
- 670 18. López-García JA, Oyarzun R, López-Andrés S, Manteca Martínez JI (2011) Scientific, edu-  
671 cational, and environmental considerations regarding mine sites and geoheritage: a perspective  
672 from SE Spain. *Geoheritage* 3:267–275
- 673 19. Oyarzun R, Manteca-Martínez JI, López-García JA, Carmona C (2013) An account of the  
674 events that led to full bay infilling with sulfide tailings at Portman (Spain), and the search for  
675 “black swans” in a potential land reclamation scenario. *Sci Total Environ* 454–455:245–249

20. Robles-Arenas VM, Rodríguez R, García C, Manteca JI, Candela L (2006) Sulphide-mining impacts in the physical environment: Sierra de Cartagena-La Unión (SE Spain) case study. *Environ Geol* 51:47–64 676
21. Navarro MC, Pérez-Sirvent C, Martínez-Sánchez MJ, Vidal J, Tovar PJ, Bech J (2008) Abandoned mine sites as a source of contamination by heavy metals: a case study in a semi-arid zone. *J Geochem Explor* 96:183–193 677
22. García-Lorenzo ML, Pérez-Sirvent C, Martínez-Sánchez MJ, Molina-Ruiz J (2012) Trace elements contamination in an abandoned mining site in a semiarid zone. *J Geochem Explor* 13:23–35 678
23. Arribas A Jr, Cunningham CG, Rytuba JJ, Rye RO, Kelly WC, Podwysoki MH, McKee EH, Tosdal RM (1995) Geology, geochronology, fluid inclusions, and isotope geochemistry of the Rodalquilar gold alunite deposit, Spain. *Econ Geol* 90:795–822 679
24. Oyarzun R, Cubas P, Higuera P, Lillo J, Llanos W (2009) Environmental assessment of the arsenic-rich, Rodalquilar gold-(copper-lead-zinc) mining district, SE Spain: data from soils and vegetation. *Environ Geol* 58:761–777 680
25. Urbano Vicente R (1998) Guía para la investigación de los recursos minerales en España (Guideline on the investigation of mineral resources in Spain). IGME, Madrid 681
26. Callender E (2004) Heavy metals in the environment-historical trends. In: Lollar BS (ed) *Treatise on Geochemistry* 9. Environmental Geochemistry, Elsevier, Amsterdam, pp 67–105 682
27. Lin Y, Tiegeng L (1999) Sphalerite chemistry, Niujiatong Cd-rich zinc deposit, Guizhou, Southwest China. *Chin J Geochem* 18:62–68 683
28. Goldschmidt V (1937) The principles of distribution of chemical elements in minerals and rocks. *J Chem Soc, March*, pp 655–673. doi:10.1039/JR9370000655 684
29. Gill R (1996) *Chemical fundamentals of geology*. Chapman and Hall, London 685
30. Oyarzun R (1976) Alteración hidrotermal y distribución de Cu, Mo, Pb y Zn en el prospecto Kilómetro Catorce, El Salvador, III Región (Hydrothermal alteration and distribution of Cu, Mo, Pb and Zn in the prospect Kilómetro Catorce, El Salvador, III Region). In: *Proceedings of the 1st Congreso Geológico Chileno, 2–7 August 1976*. Santiago, Chile, 2, E125–E143 686
31. Blanchard R (1968) Interpretation of Leached Outcrops. *Nevada Bureau of Mines Bulletin* 66 687
32. Lázaro I, Cruz R, González I, Monroy M (1997) Electrochemical oxidation of arsenopyrite in acidic media. *Int J Miner Process* 50:3–75 688
33. Morin G, Calas G (2006) Arsenic in soils, mine tailings, and former industrial sites. *Elements* 2:97–101 689
34. USEPA (2013). Drinking water contaminants. Water, United States Environmental Protection Agency. <http://water.epa.gov/drink/contaminants/index.cfm>. Accessed 10 Feb 2014. 690
35. Benjamin MM, Honeyman BD (2006) Trace Metals. In: Jacobson MC, Charlson RJ, Rodhe H, Orians GH (eds) *Earth system science, International Geophysics Series* 72. Elsevier, Amsterdam, pp 377–418 691
36. MacDonald DD, Ingersoll CG, Berger TA (2000) Development and evaluation of consensus-based sediment quality guidelines for freshwater ecosystems. *Arch Environ Contam Toxicol* 39:20–31 692
37. CCME (1999) Canadian soil quality guidelines for the protection of environmental and human health. *Canadian Environmental Guidelines*, Canadian Council of Ministers of the Environment, <http://ceqg-rcqe.ccme.ca/>. Accessed 12 Jun 2014 693
38. Manceau A, Boisset MC, Sarret G, Hazemann JL, Mench M, Cambier P, Prost R (1996) Direct determination of lead speciation in contaminated soils by EXAFS spectroscopy. *Envir Sci Technol* 30:1540–1552 694
39. Roberts DR, Scheinost AC, Sparks DL (2002) Zinc speciation in a smelter-contaminated soil profile using bulk and microspectroscopic techniques. *Envir Sci Technol* 36:1742–1750 695
40. Oyarzun R, Lillo J, Higuera P, Oyarzún J, Maturana H (2004) Strong arsenic enrichment in sediments from the Elqui watershed, Northern Chile: industrial (gold mining at El Indio-Tambo district) vs. geologic processes. *J Geochem Explor* 84:53–64 696

- 729 41. Seaman JC, Bertsch PM, Strom RN (1997) Characterization of colloids mobilized from  
730 southeastern coastal plains sediments. *Envi Sci Technol* 31:2782–2790
- 731 42. Davis JA, Kent DB (1990) Surface complexation modeling in aqueous geochemistry. In:  
732 Hochella MF, White AF (eds) *Mineral-Water Interface Geochemistry*. Reviews in Mineralogy,  
733 23, Mineralogical Society of America, Washington DC, pp 177–260
- 734 43. Smith KS (1999) Metal sorption on mineral surfaces: an overview with examples relating to  
735 mineral deposits. In: Plumlee GS, Logsdon MJ (eds) *The environmental geochemistry of  
736 mineral deposits*. Reviews in Economic Geology 6A, Society of Economic Geologists, Chel-  
737 sea, Michigan, pp 161–182
- 738 44. Smedley PL, Kinniburgh DG (2002) A review of the source, behaviour and distribution of  
739 arsenic in natural waters. *Appl Geochem* 17:517–568
- 740 45. Meng X, Korfiatis GP, Bang S, Bang KW (2002) Combined effects of anions on arsenic  
741 removal by iron hydroxides. *Toxicol Lett* 133:103–111
- 742 46. Fitz WJ, Wenzel WW (2002) Arsenic transformations in the soil-rhizosphere-plant system:  
743 fundamentals and potential application to phytoremediation. *J Biotechnol* 99:259–278
- 744 47. Ellis EC, Kaplan JO, Fuller DQ, Vavrus S, Goldewijk KK, Vervurg PH (2013) Used planet: a  
745 global history. *Proc Natl Acad Sci USA* 110:7978–7985
- 746 48. Hooke RLEB, Martin-Duque JF, Pedraza J (2012) Land transformation by humans: a review.  
747 *GSA Today* 22:4–10
- 748 49. USEPA (2012). Health. Six common pollutants, lead in air; United States Environmental  
749 Protection Agency, <http://www.epa.gov/oar/lead/health.html>. Accessed 10 Feb 2014
- 750 50. Landrigan PJ, Baker EL Jr, Feldman RG, Cox DH, Eden KV, Orenstein WA, Mather JA,  
751 Yankel AJ, Lindern IHV (1976) Increased lead absorption with anemia and slowed nerve  
752 conduction in children near a lead smelter. *J Pediatr* 89:904–910
- 753 51. Sepúlveda V, Vega J, Delgado I (2000) Exposición severa a plomo ambiental en una población  
754 infantil de Antofagasta, Chile (Childhood environmental lead exposure in Antofagasta, Chile).  
755 *Rev Med Chile* 128:221–232
- 756 52. USEPA (2005) Toxicological review of zinc and compounds. United States Environmental  
757 Protection Agency, CAS No. 7440-66-6, <http://www.epa.gov/iris/toxreviews/0426tr.pdf>.  
758 Accessed 10 Feb 2014
- 759 53. WHO (2011) Cadmium in drinking-water. Background document for development of  
760 WHO Guidelines for Drinking-water Quality, World Health Organization, WHO/SDE/WSH/  
761 03.04/80/Rev/1, [http://www.who.int/water\\_sanitation\\_health/dwq/chemicals/cadmium.pdf](http://www.who.int/water_sanitation_health/dwq/chemicals/cadmium.pdf).  
762 Accessed 10 Feb 2014
- 763 54. Bissen M, Frimmel FH (2003) Arsenic – a review. Part I: occurrence, toxicity, speciation,  
764 mobility. *Acta Hydroch Hydrob* 31:9–18
- 765 55. Edwards KJ, Schrenk MO, Hamers R, Bandfield JF (1998) Microbial oxidation of pyrite:  
766 experiments using microorganisms from an extreme acidic environment. *Am Mineral*  
767 83:1444–1453
- 768 56. Nordstrom DK, Alpers CN (1999). Geochemistry of acid mine waters. In: Plumlee GS,  
769 Logsdon MJ (eds) *Reviews in economic geology, 6A, The environmental geochemistry of  
770 mineral deposits*. Part A. Processes, methods and health issues. Society of Economic Geolo-  
771 gists, Littleton, pp 133–160
- 772 57. Oyarzun R, Lillo J, Oyarzun J, Maturana H, Higuera P (2007) Mineral deposits and Cu-Zn-As  
773 dispersion-contamination in stream sediments from the semiarid Coquimbo Region, Chile.  
774 *Environ Geol* 53:283–294
- 775 58. Nordstrom DK (2009) Acid rock drainage and climate change. *J Geochem Explor* 100:97–104
- 776 59. Singh A, Nocerino J (2002) Robust estimation of mean and variance using environmental data  
777 sets with below detection limit observations. *Chemometr Intell Lab* 60:69–86
- 778 60. Templ M, Filzmoser P, Reimann C (2008) Cluster analysis applied to regional geochemical  
779 data: problems and possibilities. *App Geochem* 23:2198–2213
- 780 61. Limpert E, Stahel WA, Abbot M (2001) Log-normal distributions across the sciences: keys and  
781 clues. *Bioscience* 51:341–352

62. Jiménez-Ballesta R, Bueno PC, Rubí JAM, Gimenez RG (2010) Pedo-geochemical baseline content levels and soil quality reference values of trace elements in soils from the Mediterranean (Castilla-La Mancha, Spain). *Central Eur J Geosci* 2:441–452 782–784
63. Galán E, Fernández-Caliani JC, González I, Aparicio P, Romero A (2008) Influence of geological setting on geochemical baselines of trace elements in soils. Application to soils of Southwest Spain. *J Geochem Explor* 98:89–106 785–787
64. Hidalgo Estévez MC, Benavente Herrera J, Rey Arrans J (1999) First results on the presence of metallic contaminants in waters after the abandonment of a sulphide mining district (Linares, Spain). In: *Proceedings of the mine, water & environment for the 21st century*, International Mine Water Association, Sevilla 788–791
65. Sánchez España J, López Pamo E, Santofimia E, Aduvire O, Reyes J, Baretino D (2005) Acid mine drainage in the Iberian Pyrite Belt (Odiel river watershed, Huelva, SW Spain): geochemistry, mineralogy and environmental implications. *App Geochem* 20:1320–1356 792–794
66. Oyarzun R, Higuera P, Lillo J (2011) *Minería Ambiental: Una Introducción a los Impactos y su Remediación* (Environmental mining: an introduction to impacts and remediation techniques). [http://www.aulados.net/Libros\\_Aula2punto.net\\_GEMM/Libros.html](http://www.aulados.net/Libros_Aula2punto.net_GEMM/Libros.html). Accessed 12 Jun 2014 795–799